Journal of Power Sources 196 (2011) 5844–5848

Contents lists available at ScienceDirect

Journal of Power Sources

journal homepage: www.elsevier.com/locate/jpowsour

Short communication

Preparation of PtNi hollow nanospheres for the electrocatalytic oxidation of methanol

Xin-Wen Zhou [a,*], Rong-Hua Zhang [a], Zhi-You Zhou [b], Shi-Gang Sun [b,*]

[a] College of Chemistry and Life Science, Department of Chemistry, China Three Gorges University, Yichang 443002, China
[b] State Key Lab for Physical Chemistry of Solid Surface, Department of Chemistry, College of Chemistry and Chemical Engineering, Xiamen University, Xiamen 361005, China

ARTICLE INFO

Article history:
Received 13 January 2011
Received in revised form 21 February 2011
Accepted 22 February 2011
Available online 5 March 2011

Keywords:
Hollow PtNi nanospheres
Successive-reduction
Methanol electrocatalytic oxidation
Fuel cell

ABSTRACT

We report the synthesis and characterization of hollow PtNi nanospheres by chemical successive-reduction method. The results of X-ray diffraction (XRD) and X-ray photoelectron spectroscopy (XPS) account for the alloy formation between Pt and Ni and electronic structure change of Pt in the alloy. The prepared nanospheres show a high activity and stability for electrocatalytic oxidation of methanol as compared to the commercial Pt/C catalyst and the co-reduced PtNi nanoparticles. The reasons of the high electrocatalytic activity of the hollow PtNi nanospheres were discussed.

1. Introduction

Magnetic platinum–nickel (PtNi) alloy nanoparticles have a potential application in high density data storage [1,2] and as catalysts [3–9]. For example, PtNi nanoparticles were frequently used in direct oxidation methanol fuel cell (DMFC) [3–5] or direct borohydride fuel cell (DBFC) [6,7] as anode catalysts, and as a cathode catalyst for electro-reduction of oxygen [8,9]. These catalytic properties are highly dependent on the size, shape and composition of the nanoparticles. Then syntheses yielding monodisperse PtNi nanoparticles with controllable morphology and composition are crucial for progress in this field [10].

Hollow metallic nanomaterials exhibit different properties from their solid counterparts with the advantages of low density, saving of material, and cost reduction. Spherical Pt and CoPt alloy electrocatalysts with a hollow structure have been reported actually for electrooxidation of methanol [11,12]. PtNi hollow spheres prepared by a template-replacement route as catalysts for hydrogen generation from ammonia borane have been investigated [13]. This method consists of the removal of the template after the synthesis, which may destroy the structure of the products.

In this communication, we report the synthesis of PtNi nanospheres with different structures by chemical successive- and co-reduction methods. The size, composition and morphology of the products are characterized in detail. The hollow PtNi particles exhibit a nearly treble improvement of electrooxidation activity of CH_3OH as compared to commercial Pt/C catalyst.

2. Experimental

2.1. Preparation of catalysts

The growth of the PtNi nanospheres was carried out through a successive-reduction and co-reduction process. In brief, 9.5 mg $NiCl_2$, 60 ml H_2O and 100 mg poly(vinylpyrrolidone) (PVP) were mixed in a three-necked flask equipped with a heat controller. The mixture was kept at 25 °C with vigorous stirring. Then, 25 ml of 0.01 M freshly prepared $NaBH_4$ solution was added slowly. Once the $NaBH_4$ is completely dropped into the solution, 20 ml of 0.4 M K_2PtCl_6 was added dropwise. To avoid oxidation of the Ni nanoparticles, high-purity N_2 was bubbled into the solution during the whole procedure. The black solution was stirred for 2 h and cooled to room temperature, then were separated, washed thoroughly and dispersed in ultrapure water for following studies. This kind product was recorded as PtNi-a. When $NiCl_2$ and K_2PtCl_6 were mixed together first, the co-reduced product was recorded as PtNi-b.

2.2. Physical characterization

The powder samples were characterized by powder X-ray diffraction (XRD) using a Panalytical X'pert PRO diffractometer. Transmission electron microscopy (TEM) patterns were obtained

* Corresponding authors. Tel.: +86 0592 2180181; fax: +86 0592 2183047.
E-mail addresses: xwzhou@ctgu.edu.cn (X.-W. Zhou), sgsun@xmu.edu.cn (S.-G. Sun).

0378-7753/$ – see front matter © 2011 Elsevier B.V. All rights reserved.
doi:10.1016/j.jpowsour.2011.02.088

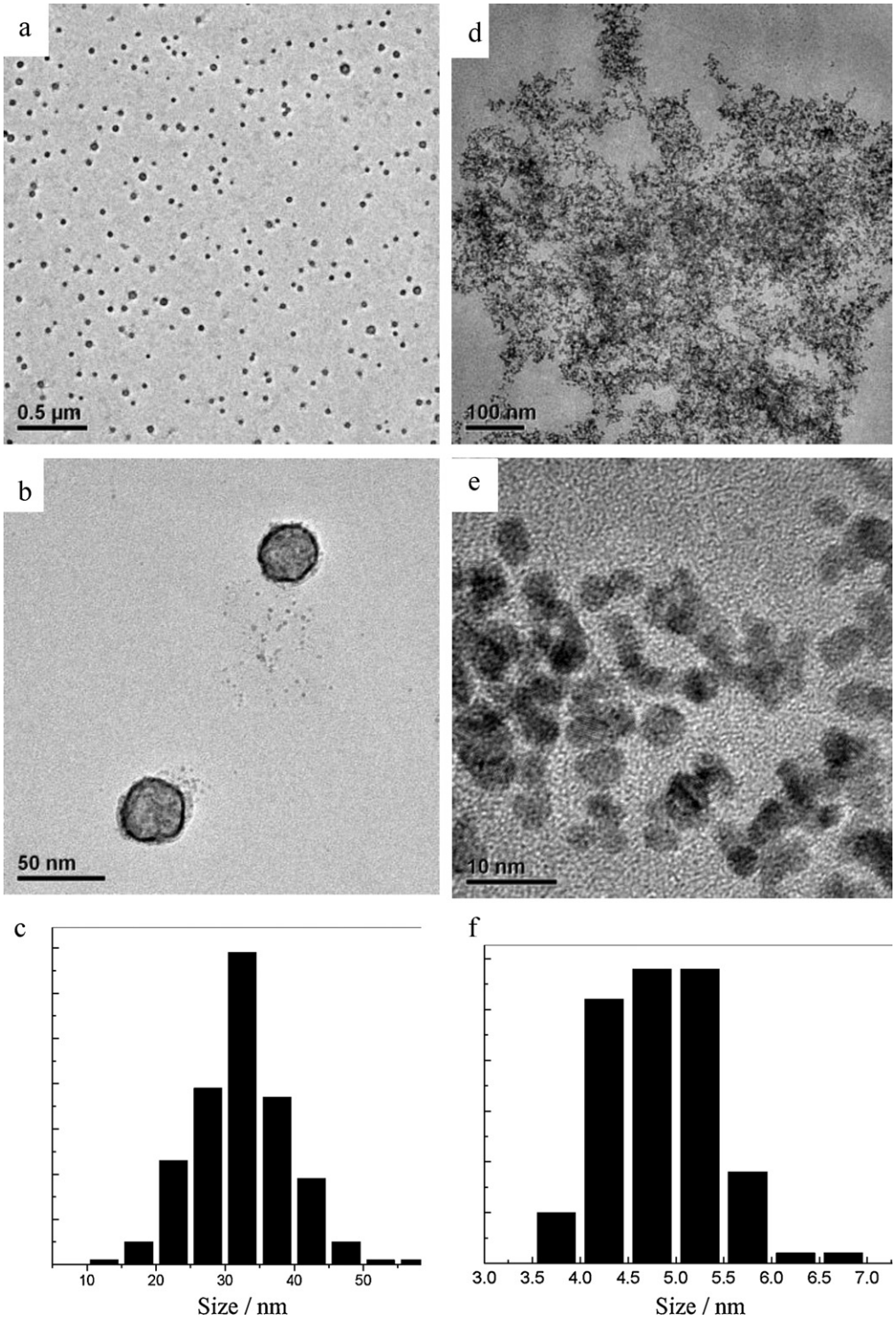

Fig. 1. TEM, high magnification TEM images and size histogram of obtained particles (a, b, c: PtNi-a; d, e, f: PtNi-b).

on instruments of FEI Tecnai-F30 electron microscopy. The samples for TEM analysis were prepared by adding a drop of the solution of PtNi nanospheres on a carbon-coated copper grid. The energy dispersive of X-ray (EDAX) was attached to the TEM system. X-ray photoelectron spectroscopy (XPS) spectrum was recorded by a PHI Quantum 2000 XPS system (Physical Electronics, Inc.) using Al Kα radiation at a base pressure below 5×10^{-8} Torr. The cyclic voltammetry (CV) studies were carried out with a CHI631C electrochemical work station (CH instruments, Inc.).

2.3. Electrochemical measurements

Electrochemical experiments were carried out in a standard three-electrode cell at room temperature. The counter electrode was a Pt flake and reference electrode was a saturated calomel electrode (SCE). A prescribed quantity of suspension of PtNi nanomaterials or commercial Pt/C catalyst (Johnson-Matthey, 20 wt% Pt) were applied to the surface of glassy carbon (GC) electrode, upon which a drop of 0.5% (v/v) Nafion solution was dispersed to fix the

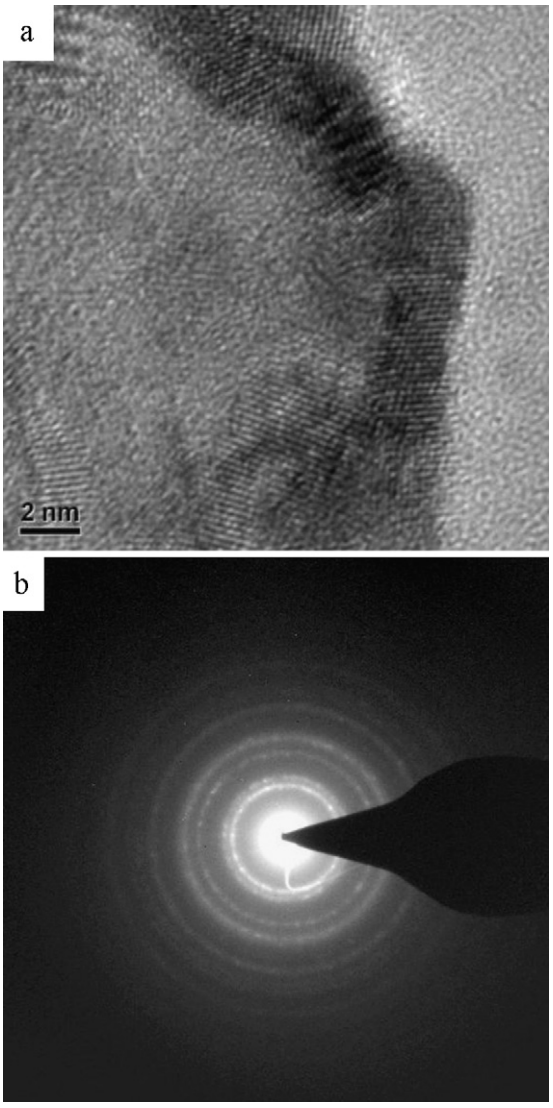

Fig. 2. (a) HRTEM and (b) SAED patterns of PtNi-a nanospheres.

particles on the surface. The electrode thus prepared is denoted thereafter as PtNi/GC or Pt/C/GC. The loading of platinum was about 1.5–4.0 μg cm^{-2}, depending on the particles density in the suspension. All electrolyte solutions were prepared using water purified by a Milli-Q system with a resistivity of 18.2 MΩ cm.

3. Results and discussion

TEM images in Fig. 1a illustrate that large-scale PtNi-a nanoparticles have been synthesized. It can be seen that the products are spherical and monodisperse with a diameter of 32.4 nm (Fig. 1c). The structural details are revealed in high-magnification TEM (Fig. 1b) and high-resolution TEM (HRTEM) images (Fig. 2a). The center portions of the nanospheres are brighter than their wall edge, illustrating a hollow structure [11–13]. The PtNi nanospheres have crystalline structures, as shown by the clear lattice fringes in the HRTEM images (Fig. 3a) and the selected area electron diffraction (SAED) pattern (Fig. 3b) [6]. The measured lattice fringe distance agrees with that reported for PtNi alloy [6,14]. The energy dispersive X-ray spectroscopy (Fig. 4a) demonstrates the coexistence of Pt and Ni with an average composition of $Pt_{70}Ni_{30}$, which is comparable to the ratio of the reactants of Pt to Ni (2:1). As shown in Fig. 1d–f, the PtNi-b nanoparticles are solid, spherical with an

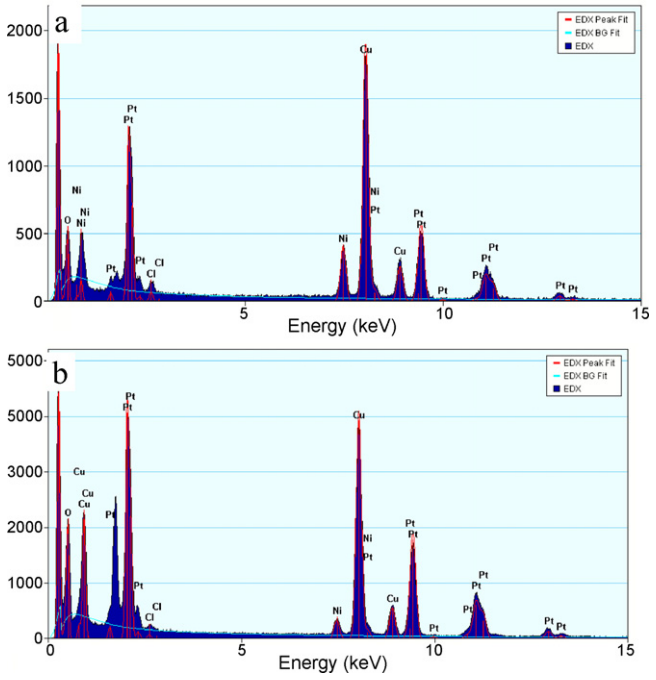

Fig. 3. EDAX of (a) NiPt-a and (b) NiPt-b nanospheres.

average diameter of 4.8 nm (Fig. 1f). We also observe that the PtNi-b nanoparticles are partly aggregated together (Fig. 1e). The results of EDAX in Fig. 4b show that the average composition of PtNi-b is about $Pt_{80}Ni_{20}$.

Fig. 4 shows the XRD patterns of the PtNi and Pt nanoparticles, in which the characteristic peaks from a crystalline face centered cubic (fcc) Pt phase appear at the corresponding diffraction angles for the (1 1 1), (2 0 0), (2 2 0), and (3 1 1) fundamental peaks. The typical *fcc*-Pt diffraction peaks in the PtNi nanoparticles seem to be broadened and there are no noticeable peaks for phase separated structures such as a pure Ni or its oxides in our XRD measurements, indicating a good degree of alloying between Pt and Ni. In particular, the diffraction peaks were slightly shifted to the high 2θ values in the PtNi particles as compared to those of the pure Pt particles, in agreement with Vegard's law [15,16].

X-ray photoelectron spectroscopy (XPS) spectrum is a useful tool to study electrocatalysts for fuel cells [6,17]. It allows

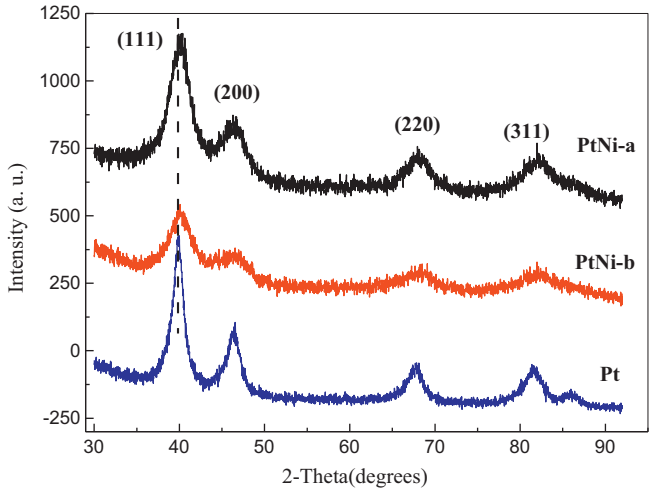

Fig. 4. XRD patterns of PtNi-a, PtNi-b and Pt nanoparticles.

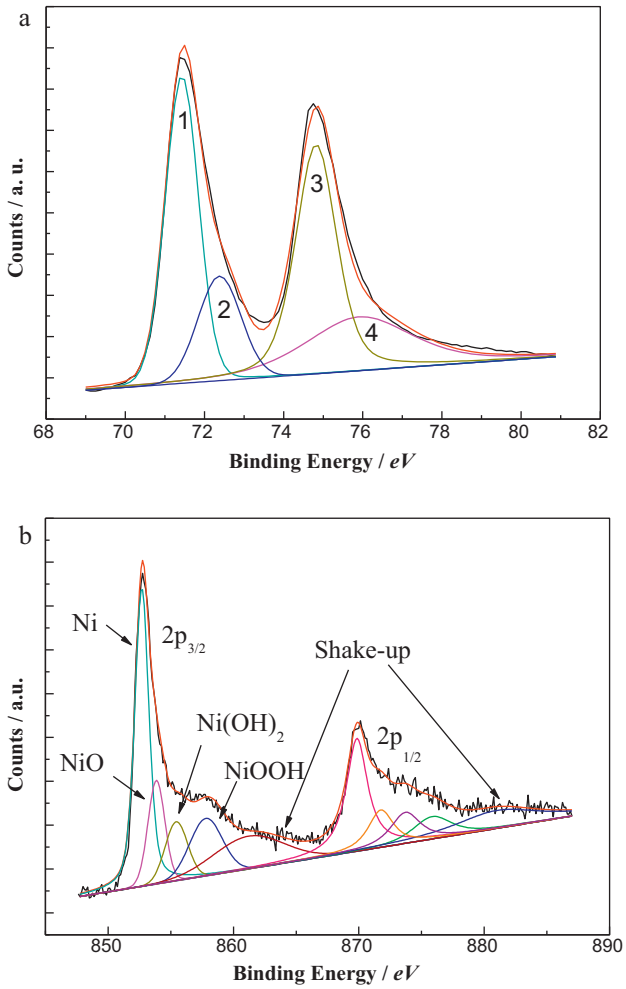

Fig. 5. XPS spectra of (a) Pt_{4f} and (b) Ni_{2p} regions of PtNi-a nanoparticles.

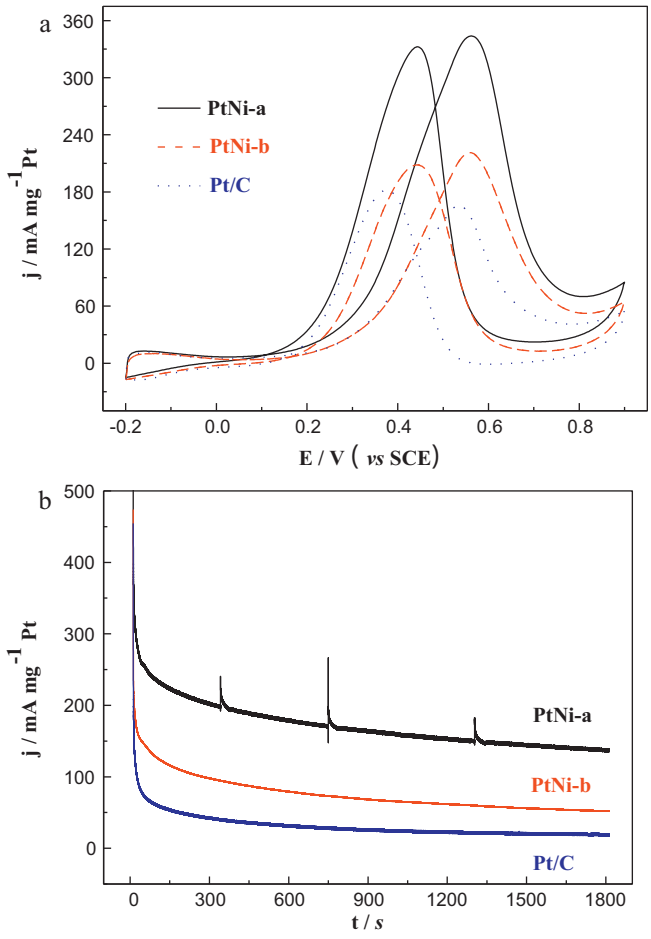

Fig. 6. (a) Cyclic voltammograms of PtNi-a/GC, PtNi-b/GC, and Pt/C/GC electrodes in 0.1 M H_2SO_4 + 0.1 M CH_3OH and (b) *j–t* curves obtained at 0.45 V with a scan rate of 50 mV s^{-1}

determination of changes in the electronic structure for different surface preparations and compositions mainly based on shifts of the binding energies of core-level electrons. Fig. 5 shows the region of Pt_{4f} and Ni_{2p} in the XPS spectrum of the PtNi-a nanoparticles. The spectrum can be fit by two pairs of overlapping Lorentzian curves [18]. The $Pt_{4f7/2}$ and $Pt_{4f5/2}$ lines appearing at 71.0 eV (peak 1) and 74.4 eV (peak 3) are attributed to metallic Pt^0. The other peaks appearing at 72.0 eV (peak 2) and 75.5 eV (peak 4) can be assigned to Pt^{2+} species in PtO and $Pt(OH)_2$ [16–20]. A comparison of the relative intensities of the peaks shows that Pt in the PtNi nanoparticles is predominately present in the zerovalent metallic state. With reference to pure Pt, the Pt_{4f} XPS spectrum of PtNi-a nanospheres experiences peak shifts negatively, which indicates an electronic stage change of Pt when it was alloyed with Ni [6]. The XPS spectrum of Ni_{2p} is shown in Fig. 5b. The Ni states consist of Ni^0, NiO, $Ni(OH)_2$ and NiOOH. In general, the $Ni_{2p3/2}$ spectrum is made complicated by the presence of satellite signals of high binding energy adjacent to the main peaks [17,21,22]. Taking the satellite peaks into account, the $Ni_{2p3/2}$ peaks at the binding energies of 852.56, 853.73, 855.87, and 857.51 eV correspond to Ni^0, NiO, $Ni(OH)_2$ and NiOOH, respectively. But in XRD studies, we could not find the peaks of the hydroxides or oxides of Ni, which is possibly because of their amorphous nature [6,17]. These Ni hydroxide layer has some favorable properties, such as proton and electronic conductivity, and stability in acidic solution.

The cyclic voltammograms of the three samples in 0.1 M H_2SO_4 containing 0.1 M CH_3OH are shown in Fig. 6a. The oxidation current has been normalized to mass-specific current density so that the current density (*j*) can be directly used to compare the catalytic activity of the samples. Both PtNi-a and PtNi-b particles examined show a significantly improved CH_3OH oxidation activity as compared to the Pt/C catalyst. The ratio of peak currents associated with the anodic peaks in forward (I_f) and reverse (I_b) is generally used to describe the tolerance of a catalyst to intermediates generated during the oxidation of methanol [23]. A low I_f/I_b ratio indicates poor electrooxidation of methanol to carbon dioxide during the forward scan, and excessive accumulation of carbonaceous intermediates on the catalyst surface [24]. For PtNi-a/C catalyst, the value of I_f/I_b was 1.04, which is larger than that of the Pt/C catalyst (0.91) and close to the PtNi-b/C (1.06) nanomaterials. The I_f/I_b value of PtNi-a catalyst is 1.14 times as that of the Pt/C catalyst. The results of the I_f/I_b ratio indicate that the hollow PtNi-a catalysts exhibits excellent poison tolerance than that of the commercial Pt/C catalyst. Fig. 6b shows a comparison of current density of CH_3OH oxidation at 0.45 V of the three samples. The oxidation current density obtained on PtNi-a particles is higher than that on Pt/C catalyst. The stability of the samples was also investigated through chronoamperometry by applying the procedure reported in our previous work [25]. The *j–t* curves of PtNi-a/GC, PtNi-b/GC and Pt/C/GC obtained at 0.45 V are compared in Fig. 5b. The current is decreased sharply in the first few seconds and then reaches a steady-state current. It can be seen that the current density of methanol oxidation on PtNi-a/GC is always larger than that on PtNi-b/GC and Pt/C/GC, evidencing the high activity and high stability of the hollow PtNi nanospheres for the electrooxidation of

CH_3OH. The enhanced CH_3OH oxidation activity was also observed on other PtNi particles and can be explained by bifunctional mechanism [19,26], the Pt electronic structure change [6] and its especial hollow structure [11–13,27].

4. Conclusions

In summary, monodisperse PtNi nanospheres with a hollow structure can be synthesized by chemical successive-reduction methods. The hollow PtNi nanospheres exhibit a superior electrocatalytic activity toward CH_3OH electrooxidation than that of commercial Pt/C catalyst. Future research will be needed to improve the synthesis technique so that smaller-size Pt-based alloy with a hollow structure will be made in high yield and decrease the content of the platinum in the catalyst.

Acknowledgements

Financial supports from Natural Science Foundation of China (20833005 and 21021002), Special Funds for Major State Basic Research Project of China (2009CB220102) are highly acknowledged.

References

[1] M. Chen, J.P. Liu, S. Sun, J. Am. Chem. Soc. 126 (2004) 8394.
[2] A. Cheng, P. Holt-Hindle, Chem. Rev. 110 (2010) 3767.
[3] F. Liu, J.Y. Lee, W.J. Zhou, J. Phys. Chem. B 108 (2004) 17959.
[4] Q. Jiang, L. Jiang, S. Wang, J. Qi, G. Sun, Catal. Commun. 12 (2010) 67.
[5] C. Zhou, F. Peng, H. Wang, H. Yu, C. Peng, J. Yang, Electrochem. Commun. 12 (2010) 1210.
[6] G. Wang, Y. Gao, Z. Wang, C. Du, J. Wang, G. Yin, J. Power Sources 195 (2010) 185.
[7] X. Geng, H. Zhang, W. Ye, Y. Ma, H. Zhong, J. Power Sources 185 (2008) 627.
[8] H. Yang, C. Coutanceau, J.M. Léger, N. Alonso-Vante, C. Lamy, J. Electroanal. Chem. 576 (2005) 305.
[9] H. Yang, J. Zhang, S. Kumar, H. Zhang, R. Yang, J. Fang, S. Zou, Electrochem. Commun. 11 (2009) 2278.
[10] T. Ghosh, B.M. Leonard, Q. Zhou, F.J. DiSalvo, Chem. Mater. 22 (2010) 2190.
[11] H.P. Liang, H.M. Zhang, J.S. Hu, Y.G. Guo, L.J. Wan, C.L. Bai, Angew. Chem. Int. Ed. 43 (2004) 1540.
[12] G. Chen, D. Xia, Z. Nie, Z. Wang, L. Zhang, J. Zhang, Chem. Mater. 19 (2007) 1840.
[13] F. Cheng, H. Ma, Y. Li, J. Chen, Inorg. Chem. 46 (2007) 788.
[14] J. Arenas-Alatorre, M. Avalos-Borja, G. Diaz, Appl. Surf. Sci. (189) (2002) 7.
[15] A.R. Denton, N.W. Ashcroft, Phys. Rev. A 43 (1991) 3161.
[16] K. Ahrenstorf, O. Albrecht, H. Heller, A. Kornowski, D. Görlitz, H. Weller, Small 3 (2) (2007) 271.
[17] C.J. Corcoran, H. Tavassol, M.A. Rigsby, P.S. Bagus, A. Wieckowski, J. Power Sources 195 (2010) 7856.
[18] X. Zhang, K.Y. Chan, Chem. Mater. 15 (2003) 451.
[19] T.C. Deivaraj, W. Chen, J.Y. Lee, J. Mater. Chem. 13 (2003) 2555.
[20] Y. Baer, P.F. Heden, J. Hedeman, M. Klasson, C. Nording, K. Siegbahn, Phys. Scr. 1 (1970) 55.
[21] I.G. Casella, M.R. Guascito, M.G. Sannazzaro, J. Electroanal. Chem. 462 (1999) 202.
[22] K.W. Park, J.H. Choi, B.K. Kwon, A.S. Lee, Y.E. Sung, J. Phys. Chem. B 106 (2002) 1869.
[23] Y.N. Wu, S.J. Liao, Z.X. Liang, L.J. Yang, R.F. Wang, J. Power Sources 194 (2009) 805.
[24] J.J. Wu, H.L. Tang, Z.H. Wan, W.T. Ma, Electrochim. Acta 54 (2009) 1473.
[25] N. Tian, Z.Y. Zhou, S.G. Sun, Y. Ding, Z.L. Wang, Science 316 (2007) 732.
[26] K.J.J. Mayrhofer, V. Juhart, K. Hartl, M. Hanzlik, M. Arenz, Angew. Chem. Int. Ed. 48 (2009) 3529.
[27] X.W. Zhou, Q.S. Chen, Z.Y. Zhou, S.G. Sun, J. Nanosci. Nanotechnol. 9 (4) (2009) 2392.